*Physicochem. Probl. Miner. Process., 61(6), 2025, 216761*

http://www.journalssystem.com/ppmp

Physicochemical Problems of Mineral Processing

ISSN 1643-1049


# Hybrid coatings based on Ni@Ag and Ag nanoparticles: Fabrication and UV-Vis sintering process

**Anna Pajor-Świerzy, Mikołaj Polak, Michał Łucki, Mikołaj Zaleski, Piotr Warszyński, Krzysztof Szczepanowicz**

Jerzy Haber Institute of Catalysis and Surface Chemistry Polish Academy of Sciences, Niezapominajek 8, 30-239 Kraków, Poland

Corresponding author: anna.pajor-siwerzy@ikifp.edu.pl (Anna Pajor-Świerzy)

**Abstract:** Metallic nanoparticles are widely used to enhance the electrical conductivity of functional materials. However, despite extensive experimental and theoretical research, further improvement of their conductive performance and the development of low-temperature fabrication processes remain necessary. In this work, we report a UV–Vis-assisted, low-temperature sintering strategy for conductive coatings composed of nickel@silver (Ni@Ag) core–shell nanoparticles and size-controlled silver nanoparticles. The hybrid paste formulation enabled a significant reduction in electrical resistivity, with smaller Ag nanoparticles (10 nm) providing the highest conductivity due to enhanced particle coalescence and improved film densification. An optimal Ag nanoparticle content of 1.5 wt% resulted in coatings with a resistivity of 16 μΩ·cm, corresponding to 46% of the bulk conductivity of nickel and exceeding the performance of undoped Ni@Ag films. This scalable and non-destructive approach offers an effective route for fabricating high-conductivity coatings at low processing temperatures. This scalable, non-destructive process offers a viable route for printed conductive circuits on heat-sensitive substrates.

***Keywords:*** core@shell nanoparticles, silver nanoparticles, UV-Vis sintering, printed materials, conductive coatings

## 1. Introduction

In recent years, the deposition of metal nanoparticles (NPs) on various substrates using printing techniques has attracted significant attention for the fabrication of conductive coatings and tracks in printed electronics (Kamyshny and Magdassi, 2019; Chandrasekaran et al., 2022). High-performance printed electronic devices require well-defined conductive structures with minimal defects, as discontinuities or poor adhesion can drastically deteriorate electrical conductivity. The performance of such printed structures depends not only on the printing process but also on the properties and composition of ink formulation, including the type and concentration of conductive filler, solvents, binders, and surfactants.

Among available conductive fillers, silver nanoparticles are the most commonly used due to their high electrical conductivity, excellent oxidation resistance, and chemical stability (Kamyshny and Magdassi, 2019; Chandrasekaran et al., 2022; Divya et al., 2022). However, silver's high cost and limited availability drive the search for alternative materials. Nickel is a promising substitute because of its low price, high hardness, and good wear resistance. Nevertheless, the main challenge associated with Ni NPs is their high susceptibility to oxidation, which significantly decreases electrical performance. To overcome this issue, core@shell structures such as Ni@Ag nanoparticles have been developed, in which a thin silver shell protects the nickel core from oxidation, combining high conductivity with improved chemical stability (Reboul et al., 2021; Pajor-Świerzy et al., 2022; Pajor-Świerzy and Szczepanowicz, 2025).

To achieve conductivity, printed metallic inks usually need to undergo sintering to remove organic components and promote interparticle fusion (Dearden et al., 2005). Conventional thermal sintering is

DOI: 10.37190/ppmp/216761

effective but limited to heat-resistant substrates such as glass or ceramics (Chandrasekaran et al., 2022; Pajor-Świerzy et al., 2022; Pajor-Świerzy and Szczepanowicz, 2025; Hussain et al., 2023; Fu et al., 2023). For flexible substrates, alternative light-induced sintering methods have been developed. Among them, laser sintering allows precise energy control but is costly and less suited for large-scale applications (Hussain et al., 2023; Sharif et al., 2022). Intense pulsed light (IPL) sintering enables short processing times but can cause damage to the printed structures if the pulse energy is too high (Martins et al., 2023). Recently, UV-assisted sintering has been proposed as a low-energy, cost-efficient alternative compatible with flexible substrates. For instance, Kim et al. (2021) obtained a resistivity of $5.44 \times 10^{-6}$ Ω·cm for Ag NP films using UV-LED irradiation, while Ning et al. (2017) reported a resistivity of $6.69 \times 10^{-8}$ Ω·m for UV-sintered Ag-based gate electrodes. Similarly, Im et al. (2025) demonstrated effective ligand removal and sintering of Au NPs using low-power UV light, achieving a conductivity of $7.0 \times 10^{6}$ S·m$^{-1}$.

One common approach to improve the conductivity of metallic nanoparticle-based materials is to increase the filler concentration in the ink formulation (Wang et al., 2016). However, excessively high nanoparticle content can lead to agglomeration, precipitation, and nozzle clogging, resulting in nonuniform printed patterns. An alternative strategy is to enhance the compactness of the printed layer to create efficient conductive pathways even at low filler concentrations (Sumirat et al., 2006). Several studies have shown that introducing a bimodal or multimodal particle size distribution improves packing density and electrical conductivity. Ding et al. (2016) demonstrated that Ag NPs with a wide size distribution formed dense, conductive networks through diffusion-driven merging. Similarly, Tang et al. (2018) and Yu et al. (2022) confirmed that smaller Ag particles can fill voids between larger ones, reducing resistivity to 98 μΩ·cm and 31.2 μΩ·cm, respectively. According to packing theory, such bimodal or trimodal systems achieve optimal conductivity (Zhong et al., 2019). Furthermore, smaller nanoparticles exhibit lower melting points due to the melting point depression effect, enhancing atomic mobility and sinterability (Xiao et al., 2006; Puri and Yang, 2007). Liu et al. (2018) reported that bimodal Ag inks (10 nm and 50 nm, 2:1 wt ratio) yielded resistivity close to bulk silver under room-temperature processing.

In this study, we propose a method to enhance the electrical conductivity of coatings based on Ni@Ag core@shell nanoparticles by introducing Ag nanoparticles of different sizes to achieve a bimodal distribution. The relationship between filler size, concentration, and the resulting electrical properties of the coatings was investigated. Additionally, the influence of different types and concentrations of wetting agents on the physicochemical behavior of the inks was analyzed through measurements of surface tension and contact angles. These studies provided insight into the wettability and spreading behavior of the formulated inks, enabling optimization of their deposition quality and uniformity on various substrates. The fabricated Ni@Ag/Ag-based conductive layers were subsequently sintered using a low-temperature UV–Vis-assisted method to demonstrate a cost-effective and substrate-friendly approach to producing conductive printed coatings.

## 2. Materials and methods

### 2.1. Materials

Nickel sulfate hexahydrate ($NiSO_4 \cdot 6H_2O$), sodium borohydride ($NaBH_4$), sodium carboxymethyl cellulose MW 90000 (NaCMC), silver nitrate ($AgNO_3$), citric acid (CA), and aminomethyl propanol (AMP) were purchased from Sigma-Aldrich (Poznań, Poland). The wetting agents Surfynol PSA 336 (acetylene-based formulated surfactant), TEGO WET KL 245 (polyether siloxane copolymer), and Zetasphere 3100 (an aqueous solution of copolymers with groups of high pigment affinity) were supplied by Evonik (Essen, Germany), while BYK-348 (a silicone surfactant) was obtained from BYK-Chemie (Wesel, Germany). An aqueous colloidal solution and nanopowder of silver nanoparticles, with average sizes of 10 nm and 150 nm, respectively, were purchased from PlasmaChem (Berlin, Germany). Distilled water used for the preparation of all solutions was obtained with the four-stage Millipore Direct-Q 5UV purification system.

### 2.2. Characterization methods

The size (hydrodynamic diameter) of Ni, Ni@Ag, and Ag nanoparticles was measured using Dynamic Light Scattering (DLS) with a Zetasizer Nano Series instrument (Malvern Instruments, Malvern,

Worcestershire, UK). Each value represents the average of three runs, with at least 10 measurements per run, conducted at 25 °C. The zeta potential of their colloidal dispersions was determined using Laser Doppler Electrophoresis (LDE) on the same instrument. Zeta potential values were obtained as the average of three runs, each consisting of at least 20 measurements, also performed at 25 °C. The contact angle measurements were performed using the sessile drop method, and the surface tension was determined using the pendant drop method, both conducted with a DSA100 analyzer (KRÜSS, Germany). An optical microscope (Hirox HR-2500E) was used to analyze the quality of the obtained coatings. The morphological properties of coatings composed of Ni@Ag NPs filled with Ag NPs were studied by scanning high-resolution field emission scanning electron microscope (SEM, JEOL JSM-7500F equipped with an energy dispersive X-ray spectroscopy system (EDS-INCA PentaFETx3), enabling qualitative and quantitative information about the elemental composition and element location/distribution. The thicknesses of such films were measured by the EDXRF technique (FISCHERSCOPE X-RAY XDL 230, Worcestershire, UK). The sheet resistance of the sintered metallic coatings was measured using the four-point probe technique, in which four equally spaced colinear Kelvin probes were brought into manual contact with the coated films to establish electrical contact, and the sheet resistance was automatically recorded (Extech Instruments, 2016). Measurements were conducted using a milliohm meter (Extech Instruments, Nashua, NH, USA). To calculate the resistivity of the sintered films, the measured sheet resistance was multiplied by the film thickness, following a commonly applied procedure for printed conductive coatings (Kamyshny et al., 2011).

### 2.3. Methodology of the fabrication of hybrid paste

During the preparation of the hybrid paste, Ni@Ag nanoparticles were synthesized in two steps: (1) preparation of an aqueous dispersion of Ni nanoparticles, and (2) formation of a silver shell on their surface. The synthesis procedure for Ni@Ag NPs was developed in our laboratory and is detailed in our previous works (Pajor-Świerzy et al., 2021; Pajor-Świerzy et al., 2022; Pajor-Świerzy et al., 2023a; Pajor-Świerzy et al., 2023b). According to this method, nickel nanoparticles were first synthesized via a chemical route that enables control over particle size and distribution. In this process, a mixture was prepared containing NaCMC (30 mL, 0.5%) as a stabilizer, $NiSO_4$ (12 mL, 5.2%) as the nickel nanoparticles precursor, citric acid (12 mL, 1.4%), and AMP (5 mL, 80%) as complexing agents. Subsequently, an aqueous solution of $NaBH_4$ (30 mL, 0.2%) was introduced into the reaction mixture using a peristaltic pump, serving as the reducing agent.

In the second step, Ni@Ag nanoparticles were formed through a transmetalation (displacement) reaction. In this approach, silver ions from the silver shell precursor ($AgNO_3$, 0.02 M, 45 mL) were reduced onto the surface of the previously synthesized Ni nanoparticles. The resulting Ni@Ag nanoparticle dispersions were then purified by a centrifugation/redispersion process (two cycles at 7000 rpm for 20 minutes each) using distilled water, to remove excess stabilizer and other residual additives.

The obtained dispersion of Ni@Ag nanoparticles (NPs) was used for paste preparation. This process involved concentrating the nanoparticles to 25 wt% through a centrifugation/redispersion step (7000 rpm, 20 minutes), followed by optimization of their wetting properties using various types (BYK 348, Surfynol PSA 336, Zetasphere 3100, and TEGO WET KL 245) and concentration of wetting agent (0.015-0.03 wt%). Subsequently, commercial silver nanoparticles of various sizes (10 and 150 nm) and concentrations (0.5–2 wt%) were added to the paste with optimal properties to form a hybrid material. To obtain a homogeneous material, the hybrid paste was subjected to ultrasonication for 30 minutes at 20 kHz.

### 2.4. Fabrication of conductive coatings based on hybrid paste

The prepared hybrid paste was deposited onto polyethylene naphthalate (PEN) substrates (Kaladex® PEN 2000, DuPont Teijin Films, Redcar, North Yorkshire, UK) with dimensions of 0.3 × 0.2 × 0.125 mm, using a bar coating technique with a K-Hand Coater (Kontech, Łódź, Poland) (RK Print Coat Instruments, 2025). Prior to coating, the substrates were sequentially cleaned with isopropanol and distilled water, followed by drying with compressed air. The deposited films, covering the entire substrate area, were dried on a hot plate at 80 °C for 15 minutes. Final sintering was carried out using

UV-Vis irradiation (Osram, Warsaw, Poland) at a wavelength of 400 nm and a power density of 2.90 mW/cm². A cooling system was employed to prevent thermal effects during irradiation. The temperature was continuously monitored during the sintering process and maintained at 28 °C.

## 3. Results and discussion

In Fig. 1, a schematic representation of the fabrication process of conductive coatings based on hybrid paste using the UV-Vis sintering method is presented. According to this scheme, Ni@Ag nanoparticles (NPs) were first synthesized by reducing silver ions onto the surface of pre-formed Ni NPs through a transmetalation process, following a procedure developed in our laboratory and previously described in our publications (Pajor-Świerzy et al., 2021; Pajor-Świerzy et al., 2022; Pajor-Świerzy et al., 2023a; Pajor-Świerzy et al., 2023b).

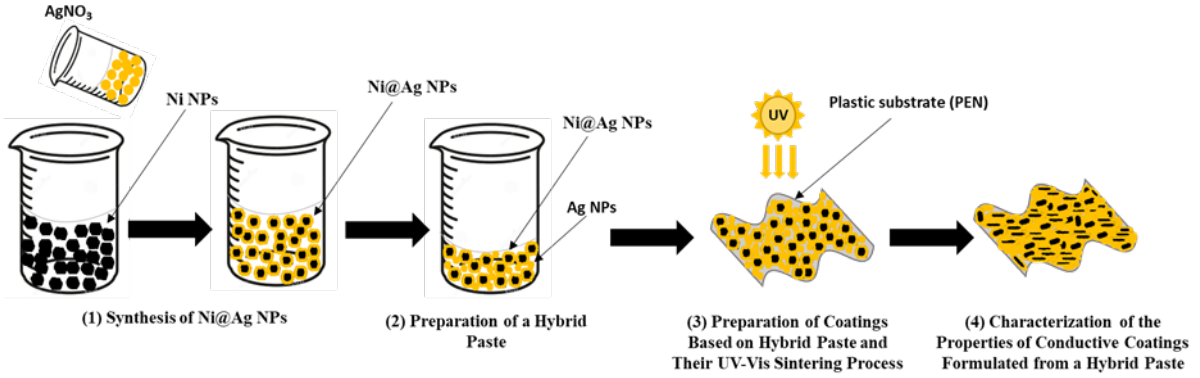


Fig. 1. Scheme of the preparation of conductive coatings based on Ni@Ag and Ag NPs on plastic substrate (PEN) by using UV-Vis sintering method

As shown by dynamic light scattering (DLS) measurements (Fig. 2A) and transmission electron microscopy (TEM) imaging (Fig. 2B), the size distribution of the synthesized Ni@Ag nanoparticles (NPs) was approximately 220 nm. The zeta potential of the Ni@Ag NPs was determined at around −35 mV, indicating good colloidal stability (O'Brien et al., 1990). The UV-Vis plasmon spectrum (Fig. 2C) of the silver-coated Ni NPs (black line) displays a characteristic silver plasmon peak at approximately 420 nm. This absorption band was not observed for bare Ni NPs, indicating the successful formation of a core@shell (Ni@Ag) structure.

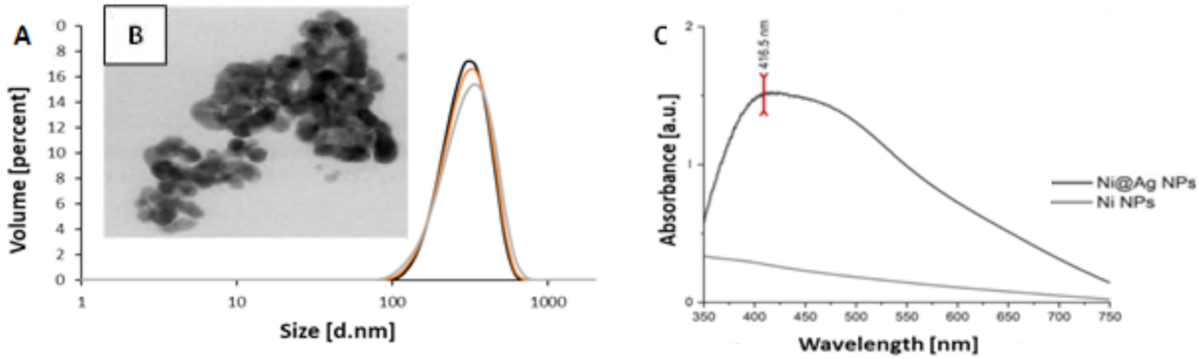


Fig. 2. Characterization of Ni@Ag NPs: (A) size distribution by volume; (B) TEM image; (C) UV-Vis spectra

Paste formulation represents a critical stage in the fabrication of conductive materials based on metallic nanoparticles. At this stage, careful control of the physicochemical properties of the formulation is required to ensure adequate interaction with the substrate. In particular, surface tension and contact angle are key parameters governing printability, as they directly affect film deposition quality and indirectly influence the electrical conductivity of the resulting layer. Both parameters are highly sensitive to paste composition. Accordingly, to achieve uniform conductive coatings on a PEN substrate, the effects of different types and concentrations of wetting agents on the surface tension and contact

angle of Ni@Ag nanoparticle-based pastes. was systematically examined. Fig. 3 presents the dependence of the paste's contact angle on PEN substrates as a function of the concentration and type of wetting agent used. A reduction in contact angle values was observed for all wetting agents. The smallest change in contact angle, from approximately 63° to 56°, was recorded with increasing concentrations of Zetasphere 3100. A more pronounced reduction in contact angle values with increasing concentration was observed for the remaining wetting agents. An increase in the concentration of TEGO WET KL 245 from 0.015 to 0.03 wt% resulted in the most significant decrease in contact angle, from 63° to approximately 12°.

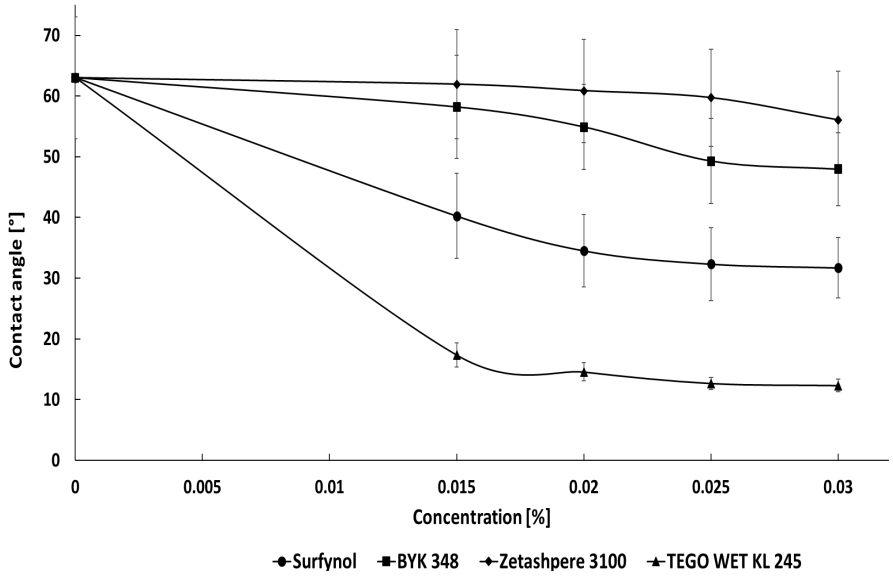


Fig. 3. The effect of the type and concentration of wetting agent on the contact angle of Ni@Ag NP-based paste deposited on a PEN substrate

Fig. 4 shows that, with increasing concentrations of all wetting agents used, the surface tension of the Ni@Ag NP-based paste gradually decreased. Similar to the changes observed in contact angle values, the smallest reduction was recorded when Zetasphere 3100 was applied, which can be attributed to its stronger role in particle redispersion rather than in improving wettability. The reduction in surface tension observed for the other types of wetting agents was comparable, with values decreasing from approximately 60 to 15–21 mN/m as the concentration increased from 0.015 to 0.03 wt%

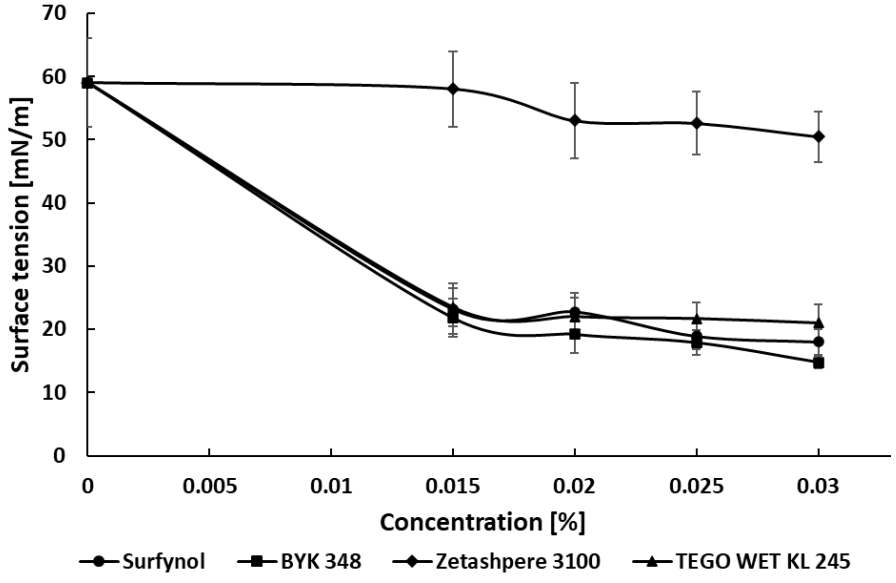


Fig. 4. The effect of the type and concentration of wetting agent on the surface tension of Ni@Ag NP-based paste

The Ni@Ag NP-based paste modified with various wetting agents was subsequently used to fabricate coatings via the bar-coating method. The high surface tension and contact angle values of the water-based formulation without any wetting agent resulted in poor-quality coatings, as shown in Fig. 5. Visual inspection and optical microscopy revealed that these films deposited on the PEN substrate were non-uniform and exhibited numerous cracks and voids. The best homogeneity was obtained for Ni@Ag films prepared from formulations containing 0.03% of each type of wetting agent. Among them, the most uniform coating was achieved using BYK-348, as can be seen in Fig. 5. This result can be attributed to its lowest surface tension value (Fig. 4) combined with an optimal contact angle (Fig. 3), which should be neither too low nor too high.

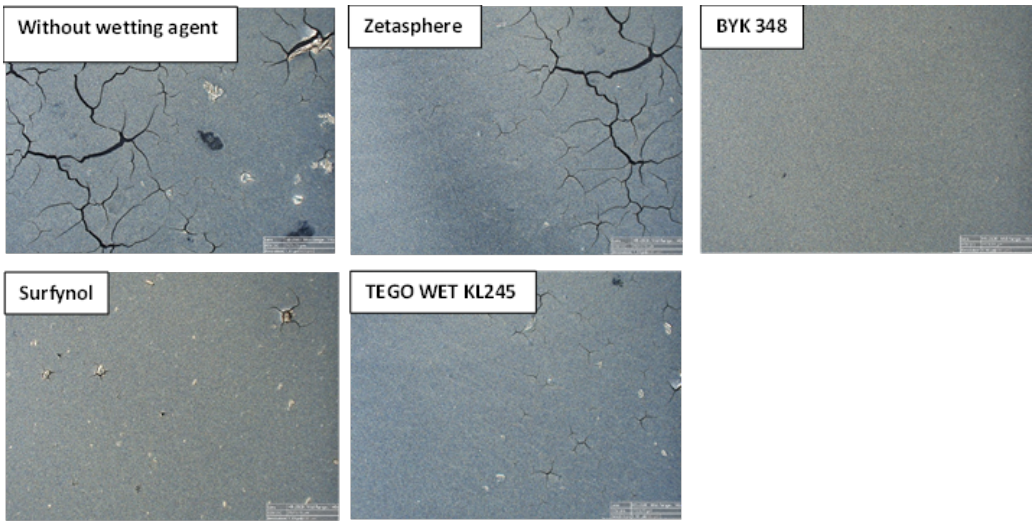


Fig. 5. Representative optical images of films obtained from Ni@Ag NP-based pastes formulated with different wetting agents at an optimal concentration of 0.03%

After optimizing the wetting properties of the Ni@Ag nanoparticle-based paste, silver nanoparticles of different average sizes were introduced to create a hybrid conductive material. The particle sizes of the commercial Ag nanoparticles were first verified by dynamic light scattering (DLS). Nanoparticles with sizes of approximately 10 nm and 150 nm were detected, consistent with the specifications provided by the manufacturer. Such silver nanoparticles were incorporated into the Ni@Ag NP-based paste at concentrations ranging from 0.5 wt% to 3 wt%. Following deposition and solvent evaporation, the hybrid coatings were subjected to UV–Vis sintering at the optimal wavelength of 400 nm for 90 min, as determined in our previous studies (Pajor-Świerzy et al., 2023a).

It is important to highlight the distinguishing features of the proposed UV–Vis-assisted sintering strategy compared to existing photonic and plasmonic sintering methods documented in the literature (Sharif et al., 2022; Kim et al., 2021; Altay et al., 2021). Unlike ultrashort laser sintering, which requires high-power lasers and can induce localized overheating (Sharif et al., 2022), our method operates at a low temperature (~28 °C) and provides uniform energy distribution across the coating, avoiding substrate damage. Similarly, high-power UV-LED sintering has been applied to silver thin films, achieving good conductivity but often with limited penetration depth and moderate scalability (Kim et al., 2021). One-step photonic curing of Ni-based inks on flexible substrates has demonstrated feasibility for printed electronics (Altay et al., 2021); however, these approaches usually require precise control of pulse duration and often do not reach the same low resistivity values achieved in our Ni@Ag/Ag hybrid coatings (~14 μΩ·cm). This demonstrates that the UV–Vis-assisted approach combines low thermal budget, high electrical performance, and compatibility with flexible substrates, addressing limitations reported in prior studies.

Furthermore, the method provides reproducibility by controlling key parameters such as wavelength, irradiation intensity, exposure time, and thermal history, which are critical for achieving consistent sintering results (Im et al., 2025; Kim et al., 2021). Previous studies on flash-light sintering of Ni nanoparticles (Park and Kim, 2014) or laser digital patterning of NiOx thin films (Nam et al., 2019) report higher resistivity (~76 μΩ·cm and sheet resistances of 53 Ω/sq, respectively) and limited

flexibility, highlighting the superior performance of the current UV–Vis-assisted process. Additionally, the approach leverages photonic and plasmonic effects, similar to those observed in gold nanoparticles (Im et al., 2025), to enhance local atomic diffusion and coalescence, further improving network connectivity and conductivity.

Fig. 6 presents the influence of Ag nanoparticle size and concentration on the resistivity of Ni@Ag NP-based coatings after UV–Vis treatment. The incorporation of Ag NPs resulted in a pronounced reduction in resistivity compared to undoped coatings, which can be attributed to the formation of additional conductive pathways provided by the highly conductive Ag domains within the hybrid coating. For both nanoparticle sizes, resistivity decreased progressively with increasing Ag NP concentration from 0.5 wt% to 2 wt%. However, a further increase in Ag NP content to 3 wt% had a negligible effect on the electrical resistivity of the Ni@Ag-based coatings. Systematic variation of the Ag nanoparticle concentration further revealed that the optimal loading of 2 wt% provided the most favorable balance between conductivity improvement and ink stability. At lower concentrations (0.5–1.5 wt%), the number of Ag particles was insufficient to form continuous conductive bridges between Ni@Ag cores, leading to higher resistivities. Conversely, further increases beyond 2 wt% (up to 3 wt%) did not yield a statistically significant improvement in electrical performance, likely due to particle aggregation and partial disruption of the uniform network structure. At the optimal Ag NP loading of 2 wt%, the resistivity was reduced from approximately 24 μΩ·cm to 14 μΩ·cm and 19 μΩ·cm for coatings containing nanoparticles with mean diameters of 10 nm and 150 nm, respectively.

The greater reduction in resistivity observed for coatings containing smaller (10 nm) Ag nanoparticles can be attributed not only to their lower melting point, which promotes more efficient particle coalescence, but also to enhanced photonic effects during UV–Vis irradiation. Under irradiation, Ag nanoparticles act as photoactive centers where electrons are excited to higher energy states. These energetic electrons may persist for several picoseconds, as previously reported for Au nanoparticles (Im et al., 2025). The photoexcited electrons facilitate local energy transfer and promote atomic diffusion at interparticle interfaces, effectively accelerating the sintering process even at relatively low temperatures. Consequently, smaller Ag nanoparticles, due to their higher surface-to-volume ratio and enhanced light absorption efficiency, enable the formation of more compact and densely connected conductive networks within the Ni@Ag/Ag hybrid coatings, resulting in significantly improved electrical conductivity.

Based on these results, the formulation containing 2 wt% of 10 nm Ag nanoparticles was selected for further investigations. Morphological evidence supporting this mechanism is provided in Fig. 8. After UV–Vis sintering at 400 nm for 90 min, Ni@Ag-based coatings doped with 2 wt% of 10 nm Ag nanoparticles underwent pronounced morphological transformations involving coalescence, surface melting, and subsequent fusion into larger metallic agglomerates. This process led to the elimination of interparticle voids and the formation of continuous, densely packed conductive pathways throughout the coating. Such structural reorganization is a result of the sintering process, where localized heating and plasmonic excitation of Ag domains promote enhanced atomic diffusion at particle interfaces. The resulting interconnected metallic framework effectively facilitates electron transport, thereby accounting for the significant improvement in the electrical performance of the Ni@Ag/Ag hybrid coating observed under these optimized UV–Vis processing conditions.

The influence of sintering time on the resistivity of coatings composed of Ni@Ag NPs doped with 2 wt% of 10 nm Ag NPs was further investigated at the optimal wavelength of 400 nm, with the results shown in Fig. 7. As shown, the optimal sintering time was confirmed as 90 min, beyond which no further improvement in coating resistivity was observed. Under these conditions, films with a resistivity of 14 μΩ·cm were obtained, corresponding to approximately 50% of the electrical conductivity of bulk nickel. This represents a marked improvement compared to our previous findings (Pajor-Świerzy et al., 2023a), in which coatings sintered under the same UV–Vis conditions but without Ag NP doping exhibited a conductivity of only 31% relative to bulk nickel.

For comparison, coatings prepared solely from Ag nanoparticles (using the same optimal concentration of BYK 348) exhibited significantly lower resistivities of approximately 2.5 μΩ·cm and 5.4 μΩ·cm for particles with mean diameters of 10 nm and 150 nm, respectively, confirming the inherently superior conductivity of pure silver-based systems. However, the high material cost of Ag

nanoparticles, combined with their susceptibility to sintering-induced coalescence and limited mechanical stability, greatly constrains their practical applications.

In this context, the Ni@Ag/Ag hybrid coatings developed in this study represent a cost-effective alternative, achieving conductivity levels approaching those of pure silver films while significantly reducing silver consumption and maintaining favorable processing and substrate compatibility. This demonstrates that the proposed Ni@Ag/Ag hybrid system provides an effective compromise between electrical performance and economic feasibility, offering a promising route toward scalable, low-cost conductive coatings for printed and flexible electronics.

In the published literature, fabrication processes of conductive coatings based on Ni@Ag NPs doped with Ag NPs using the UV–Vis sintering approach have not yet been reported. The most comparable work involves Ni NP-based films prepared by Park and Kim (2014), who optimized flash-light sintering parameters such as light energy and pulsed light patterns to produce coatings with a resistivity of 76.34 μΩ·cm, significantly higher than that achieved in the present study (~14 μΩ·cm). Photonic curing of screen-printed Ni flake ink on solid bleached sulphate (SBS) paperboard and polyethylene terephthalate (PET) substrates has also been reported (Altay et al., 2021), yielding minimum sheet resistances of 4 Ω/sq on SBS and 16 Ω/sq on PET. Furthermore, Nam et al. (2019) fabricated Ni-based flexible transparent conductive panels with sheet resistances of 53 Ω/sq on various substrates via laser digital patterning of solution-processed NiOx thin films. However, direct comparison of the sheet resistance values reported in these studies with the resistivity values obtained in this study is challenging, as the thicknesses of the reported films were not specified.

Overall, the superior performance of the developed coatings can be attributed to the synergistic effect of the silver shell and fine Ag dopants, which together facilitate efficient electron transport through a hierarchically organized conductive network. This work introduces a novel strategy for photonic sintering of hybrid metallic nanostructures with tailored microstructure and high electrical performance, thereby expanding the potential of Ni@Ag-based systems for flexible and printed electronic applications.

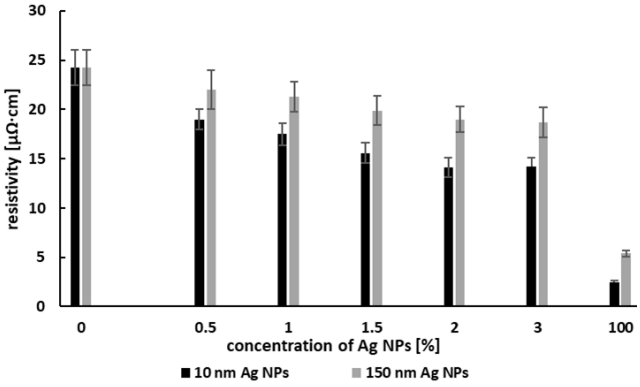


Fig. 6. The dependence of the resistivity of coatings composed of Ni@Ag NPs on the size and concentration of Ag NPs

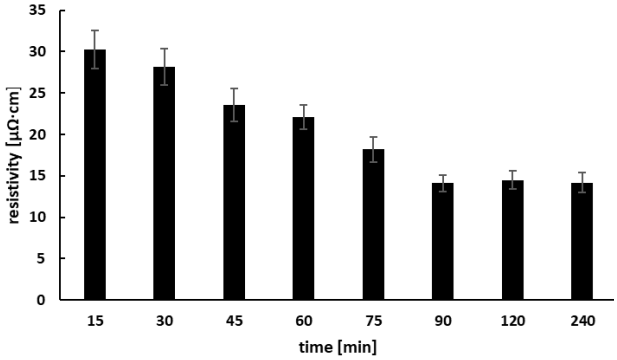


Fig. 7. Dependence of resistivity on sintering time for coatings composed of Ni@Ag NPs doped with 2% of 10 nm Ag NPs. Samples were subjected to UV–Vis sintering at the optimal wavelength of 400 nm

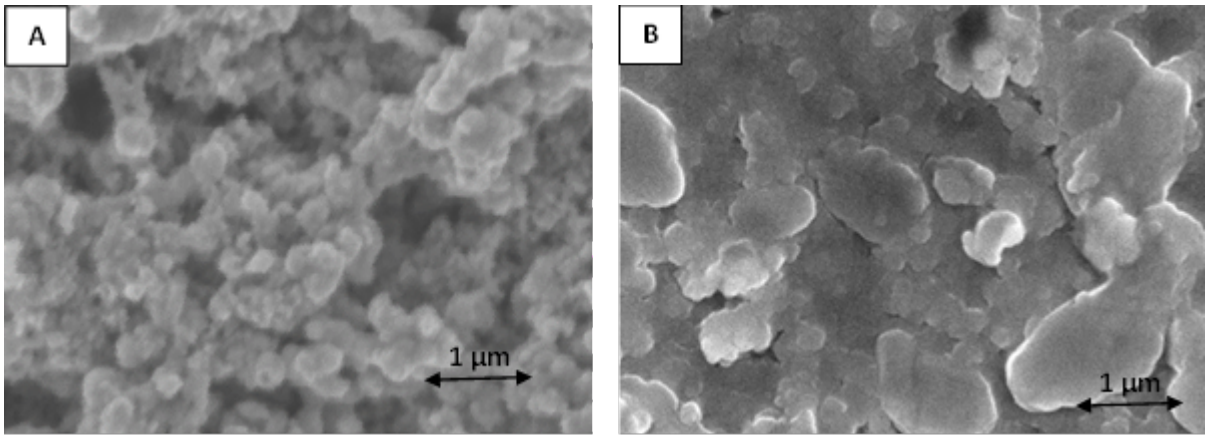


Fig. 8. Examples of SEM images of Ni@Ag NP-based coatings with 2% 10 nm Ag NPs deposited on PEN substrate: (A) after drying process (80 °C, 15 min); (B) after UV-Vis sintering at optimal conditions (90 min, 400 nm)

## 4. Conclusions

In summary, the present study introduces an efficient strategy for improving the electrical performance of Ni@Ag-based conductive coatings through the incorporation of bimodal Ag nanoparticle fillers and low-temperature UV–Vis-assisted sintering. The synergistic effect of the Ag shell and photoactive Ag nanoparticles enabled the formation of densely packed and well-connected metallic networks, resulting in a significant reduction of resistivity to 14 μΩ·cm, approximately 50% of the conductivity of bulk nickel. The demonstrated enhancement arises from the combined influence of optimized surface chemistry, controlled particle size distribution, and the photonic activation of Ag domains, which collectively promote enhanced sintering dynamics under mild conditions. This work represents, to the best of our knowledge, the first successful demonstration of UV–Vis-assisted sintering applied to hybrid Ni@Ag/Ag systems. The proposed approach offers a substrate-friendly and cost-effective route toward the fabrication of conductive coatings, holding strong potential for future applications in flexible and printed electronic devices.

## Acknowledgments

This research was funded by the National Science Centre, Poland (grant No. 2020/39/D/ST5/01937), and was partially supported by the European Union's Horizon 2020 research and innovation programme under the Marie Skłodowska-Curie Actions (grant agreement No. 955612) and by the International Fine Particle Research Institute (IFPRI).

### References

ALTAY, B.N., TURKANI, V.S., PEKAROVICOVA, A., FLEMING, P.D., ATASHBAR, M.Z., BOLDUC, M., CLOUTIER, S.G., 2021. *One-step photonic curing of screen-printed conductive Ni fake electrodes for use in flexible electronics.* Sci. Rep. 11, 3393.

CHANDRASEKARAN, S., JAYAKUMAR, A., VELU, R., 2022. *A comprehensive review on printed electronics: a technology drift towards a sustainable future.* Nanomaterials 12, 4251.

DEARDEN, A.L., SMITH, P.J., SHIN, D.-Y., REIS, N., DERBY, B., O'BRIEN, P., 2005. *A low curing temperature silver ink for use in ink-jet printing and subsequent production of conductive tracks.* Macromol. Rapid Commun. 26, 315–318.

DING, J., LIU, J., TIAN, Q., WU, Z., YAO, W., DAI, Z., LIU, L., WU, W., 2016. *Preparing highly conductive patterns on flexible substrates by screen printing of silver nanoparticles with different size distribution.* Nanoscale Res. Lett. 11, 412.

DU, T., TANG, C., XING, B., LU, Y., HUANG, F., ZUO, C., 2018. *Conductive ink prepared by microwave method: effect of silver content on the pattern conductivity.* J. Electron. Mater. 47, 231–237.

EXTECH INSTRUMENTS, 2016. *Milliohm meters.* Available online.

FU, Q., LI, W., KRUIS, F.E., 2023. *Highly conductive copper films prepared by multilayer sintering of nanoparticles synthesized via arc discharge.* Nanotechnology 34, 225601.

HONGLONG, N., ZHOU, Y., FANG, Z., YAO, R., TAO, R., CHEN, J., CAI, W., ZHU, Z., YANG, C., WEI, J., WANG, L., PENG, J., 2017. *UV-cured inkjet-printed silver gate electrode with low electrical resistivity.* Nanoscale Res. Lett. 12, 546.

HUSSAIN, A., LEE, H.L., MOON, S.J., 2023. *Sintering of silver nanoparticle structures and the pursuit of minimum resistivity.* Mater. Today Commun. 34, 105159.

IM, J., CHARLES, H., PUTRI, N.R.E., LIU, C., USUBA, J., BUTLER, K., FAY, M., GRACE, G.D.H., HOOSHMAND, H., THOMPSON, A., WILDMAN, R., HAGUE, R., TURYANSKA, L., TUCK, C., 2025. *On-demand sintering of gold nanoparticles via controlled removal of o-nitrobenzyl thiol ligands under record-low power for conductive patterns.* Adv. Sci. 12, 2415496.

KAMYSHNY, A., MAGDASSI, S., 2019. *Conductive nanomaterials for 2D and 3D printed flexible electronics.* Chem. Rev. 48, 1712–1740.

KAMYSHNY, A., STEINKE, J., MAGDASSI, S., 2011. *Metal-based inkjet inks for printed electronics.* Open Appl. Phys. J. 4, 19–36.

KIM, M., JEE, H., LEE, J., 2021. *Photo-sintered silver thin films by a high-power UV-LED module for flexible electronic applications.* Nanomaterials 11, 2840.

LIU, Z., JI, H., WANG, S., ZHAO, W., HUANG, Y., FENG, H., WEI, J., LI, M., 2018. *Enhanced electrical and mechanical properties of printed bimodal silver nanoparticle ink for flexible electronics.* Phys. Status Solidi A 215, 1800007.

MARTINS, P., PEREIRA, N., LIMA, A.C., GARCIA, A., MENDES-FILIPE, C., POLICIA, R., CORREIA, V., LANCEROS-MENDEZ, S., 2023. *Advances in printing and electronics: from engagement to commitment.* Adv. Funct. Mater. 33, 2213744.

NAM, V.B., SHIN, J., YOON, Y., GIANG, T.T., KWON, J., SUH, Y.D., YEO, J., HONG, S., KO, S.H., LEE, D., 2019. *Highly stable Ni-based flexible transparent conducting panels fabricated by laser digital patterning.* Adv. Funct. Mater. 29, 1806895.

O'BRIEN, R.W., MIDMORE, B.R., LAMB, A., HUNTER, R.J., 1990. *Electroacoustic studies of moderately concentrated colloidal suspensions.* Faraday Discuss. Chem. Soc. 90, 301–312.

PAJOR-ŚWIERZY, A., KOZAK, K., DURACZYŃSKA, D., WIERTEL-POCHOPIEŃ, A., ZAWAŁA, J., SZCZEPANOWICZ, K., 2023b. *Silver shell thickness-dependent conductivity of coatings based on Ni@Ag core–shell nanoparticles.* Nanotechnol. Sci. Appl. 16, 73–84.

PAJOR-ŚWIERZY, A., PAWŁOWSKI, R., SOBIK, P., KAMYSHNY, A., SZCZEPANOWICZ, K., 2022. *Effect of oxalic acid treatment on conductive coatings formed by Ni@Ag core–shell nanoparticles.* Materials 15, 305.

PAJOR-ŚWIERZY, A., SZYK-WARSZYŃSKA, L., DURACZYŃSKA, D., SZCZEPANOWICZ, K., 2023a. *UV–Vis sintering process for fabrication of conductive coatings based on Ni–Ag core–shell nanoparticles.* Materials 16, 7218.

PAJOR-ŚWIERZY, A., STAŚKO, D., PAWŁOWSKI, R., MORDARSKI, G., KAMYSHNY, A., SZCZEPANOWICZ, K., 2021. *Polydispersity vs. monodispersity: how the properties of Ni–Ag core–shell nanoparticles affect the conductivity of ink coatings.* Materials 14, 2304.

PAJOR-ŚWIERZY, A., SZCZEPANOWICZ, K., 2025. *The recent progress on Nickel@Silver metal core–shell nanoparticles application in printed conductive materials – a mini-review.* Nanotechnol. Sci. Appl. 18, 197–210.

PAJOR-ŚWIERZY, A., SZCZEPANOWICZ, K., KAMYSHNY, A., MAGDASSI, S., 2022. *Metallic core–shell nanoparticles for conductive coatings and printing.* Adv. Colloid Interface Sci. 299, 102578.

PARK, S.-H., KIM, H.-S., 2014. *Flash light sintering of nickel nanoparticles for printed electronics.* Thin Solid Films 550, 575–581.

PURI, P., YANG, V., 2007. *Effect of particle size on melting of aluminum at nano scales.* J. Phys. Chem. C 111, 11776–11783.

REBOUL, J., LI, Z.Y., YUAN, J., NAKATSUKA, K., SAITO, M., MORI, K., YAMASHITA, H., XIA, Y., LOUIS, C., 2021. *Synthesis of small Ni-core–Au-shell catalytic nanoparticles on $TiO_2$ by galvanic replacement reaction.* Nanoscale Adv. 3, 823–835.

RK PRINT COAT INSTRUMENTS, 2025. *K hand coater, pre-press equipment.* Available online.

SHARIF, A., FARID, N., O'CONNOR, G.M., 2022. *Ultrashort laser sintering of metal nanoparticles: a review.* Results Eng. 16, 100731.

SUMIRAT, I., ANDO, Y., SHIMAMURA, S., 2006. *Theoretical consideration of the effect of porosity on thermal conductivity of porous materials.* J. Porous Mater. 13, 439–443.

WANG, F., MAO, P., HE, H., 2016. *Dispensing of high concentration Ag nanoparticle ink for ultra-low resistivity paper-based writing electronics.* Sci. Rep. 6, 21398.

XIAO, S., HU, W., YANG, J., 2006. *Melting temperature: from nanocrystalline to amorphous phase.* J. Chem. Phys. 125, 184504.

YU, Z., ZHANG, T., LI, K., HUANG, F., TANG, C., 2022. *Preparation of bimodal silver nanoparticle ink based on liquid phase reduction method.* Nanomaterials 12, 560.

ZHONG, X.C., FENG, X.L., HUANG, J.H., JIAO, D.L., ZHANG, H., QIU, W.Q., LIU, Z.W., RAMANUJAN, R.V., 2019. *A bimodal particle size distribution enhances mechanical and magnetocaloric properties of low-temperature hot-pressed Sn-bonded La0.8Ce0.2(Fe0.95Co0.05)11.8Si1.2 bulk composites.* J. Magn. Magn. Mater. 469, 133–13.